

Multiphase flow regime transition in vertical flow

Udara S. P. R. Arachchige, Kohilan Rasenthiran, Lakshan M.A.L, Lakshitha Madalagama
M. K, Prabhath Pathirana P.R, Sakuna Sandupama P.W

Faculty of Technology
University of Sri Jayewardenepura
Nugegoda, Sri Lanka
udara@sjp.ac.lk

Received May 2019; revised May 2019

ABSTRACT. *The objective of this project is to characterize flow regimes in air-water two-phase flow based on pressure and density measurements and find the criteria for the transition between flow regimes using pressure and density parameters. Time series analysis of the liquid holdup and pressure differences, as well as video recording and visual observation, has been used to characterize the flow regime and find boundary condition for flow regime transition. The average liquid hold up at the bottom of the riser should be in the range of 0.62-0.72, and the pressure difference is approximately 107 mbar. If both of the above conditions are satisfied, then the flow regime should be a slug.*

Keywords: Bubble flow, Flow pattern, Flow regime, Multiphase flow, Slug flow

1. Introduction. Multiphase flow has become increasingly important in a wide variety of engineering systems for their optimum design and safe operations. The physical understanding of multiphase flow characteristics in vertical and horizontal pipes is of importance in the petroleum industry. The description of the two-phase flow in tubes is complicated by the existence of an interface between the two phases. For gas-liquid two-phase flows, this interface exists in a wide variety of forms, depending on the flow rates, physical properties of the phases and also on the geometry of the pipe. The different interfacial structures are called flow pattern or flow regimes [1].

Horizontal flow regimes: Bubble, Slug, Plug, Annular, Stratified, Dispersed, Wavy

Vertical flow regimes: Bubble, Slug, Churn, Annular, Disperse

Flow regime transition from one flow pattern to another is occurring because of instability.

There are several reasons for instability. Factors affecting flow regime transitions can be described as the flow rate of gas and liquid, pressure drop, pipe diameter, inclination and viscosity of the liquids [2].

Flow regime transition is very important in the multiphase flow because of [3],

- . The stable flow pattern is better for oil and gas transfer systems
- . To improve the efficiency of the plant
- . To reduce the production cost
- . To identify the suitable parameter values for operation

A particular type of geometric distribution of the components is called the flow regime or flow pattern [4]. Normally, flow regimes are recognized by visual inspection. The main flow regimes in horizontal and vertical pipes are discussed in the following sections.

Bubble flow

In this type of flow, the liquid is continuous and there is a dispersion of bubbles within the liquid. Bubble flow usually occurs at a very high liquid velocity and low gas velocity i.e. the liquid flow rate is high enough to break up the gas into bubbles but not enough to cause the bubbles to become mixed well in the liquid phase. This type of flow is characterized by the presence of fast rising bubbles with a diameter equal to or less than the capillary diameter [5]. The bubbles are often spherical or spherical-like in shape.

Dispersed bubble

This flow regime can be identified by a discontinuous gas phase distributed as spherical discrete bubbles in a continuous liquid phase. These discrete gas bubbles do not exhibit significant slippage through the liquid phase, due to the high liquid phase velocities. Thus dispersed bubble flow can be treated as a non-slip homogeneous mixture flow. This type of flow pattern occurs at low to medium superficial gas velocities with high superficial liquid velocities [5].

Slug or plug

In this type of flow, the liquid-rich slugs spread in the entire channel of the pipe. The bubbles are coalesced to make larger bubbles which approach the diameter of the tube. Slug flow pattern can be characterized by the alternate flow of gas and liquid. There are two different forms in the gas phase: large bullet shaped bubbles called Taylor bubbles and

small spherical bubbles dispersed in the liquid phase. For high flow rates, when the liquid is aerated with gas bubbles, the flow is designed as slug flow. Slug is the highly complex type flow with an unsteady nature.

Churn flow

Churn flow regime occurs in the vertical pipe after the breakdown of slug flow as the velocity of the gas increases. Changes from continuous liquid flow to continuous gas flow consist of very long gas bubbles and relatively small liquid slugs.

Annular flow

When the gas velocity is sufficiently high, the liquid in the middle of the pipe is pushed to the wall by the gas phase to form the annular flow. In this type of flow, liquid flows on the wall of the tube as a film and the gas is flowing in the middle of the tube. The liquid phase flow wetting the boundary wall and small droplets can also be seen in the middle with gas. The gas and liquid droplets flowing in the core can be assumed to be a homogeneous mixture due to the high velocity of the gas phase.

Stratified flow

Stratified flow is considered prior to the transition to slug flow regimes. Stratified flows are formed because of two superposed layers of gas and liquid segregation under the influence of gravity. This flow pattern is frequently encountered in the petroleum and chemical processing industries. Stratified flow is an intermediate regime, between a separated and a dispersed/annular flow regime, which shares some features with both of them [6].

Wavy flow

Wavy stratified flow is established in the pipeline transportation of gas-rich two-phase mixtures. By increasing the gas flow rate (at a fixed liquid rate), the interaction between fast-moving gas and the liquid layer at the bottom causes droplet entrainment.

The sketches of the flow regimes for air-water mixtures for horizontal and vertical pipes are shown in Figure 1 and Figure 2 respectively.

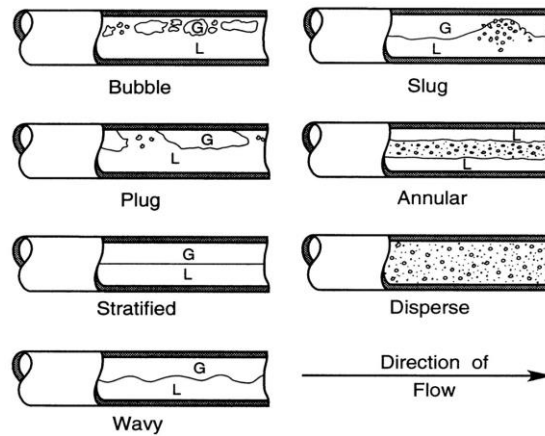


FIGURE 1. Sketches of flow regimes for air/water mixtures in a horizontal, 5.1 cm diameter pipe [4].

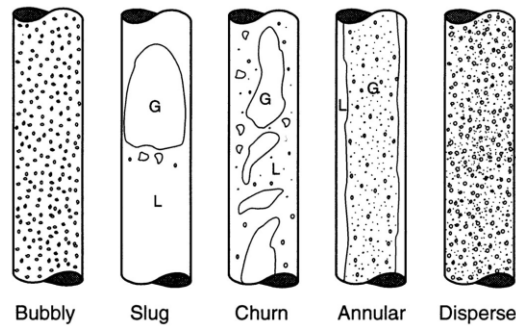


FIGURE 2. Sketches of flow regimes for two-phase flow in a vertical pipe [4].

Flow regime map

For horizontal and vertical flows, number of investigations has been conducted to determine the dependence of the flow regime on component volume fluxes, on volume fraction and on the fluid properties such as density, viscosity and surface tension. The results are displayed in the form of figure called flow regime map that identified the flow regime occurring in the various parts of a parameter space defined by the component flow rates [4]. The boundary between the various flow regimes in a flow regime map occur because a regime becomes unstable as the boundary is approached and growth of this instability causes transition to another regime.

Horizontal flow regime maps

As discussed in the previous section it is useful to provide some examples of flow regime maps along with the definitions that help distinguish the various regimes. Among various

types of regime maps, it can be seen the flows of mixtures of gas and liquid in horizontal and vertical tubes as these flows are of considerable industrial interest.

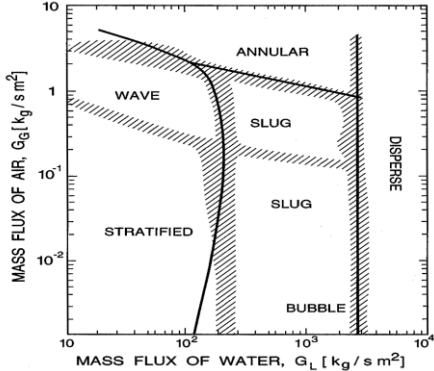


FIGURE 3. Flow regime map for the horizontal flow of an air-water mixture in a 5.1 cm diameter pipe [4].

Figure 3 shows the occurrence of different flow regimes for the flow of an air-water mixture in a horizontal, 5.1 cm diameter pipe where the regimes are distinguished visually. Christopher, E.B. (2005) has observed the hatched regions for regime boundaries close to theoretical prediction lines. There are many industrial processes in which the mass flux is a key flow parameter and therefore mass flux maps are often preferred. Other examples of flow regime maps for horizontal air-water flow (by different investigators) are shown in Figure 4 .

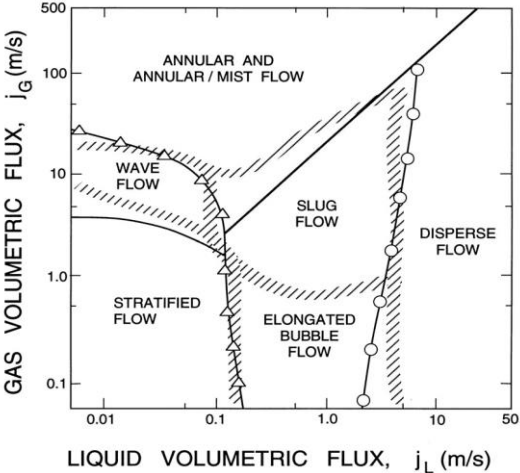


FIGURE 4. A flow regime map for the flow of an air/water mixture in a horizontal, 2.5 cm diameter pipe at 25°C and 1bar. Solid lines and points are experimental observations of the transition conditions while the hatched zones represent theoretical predictions[4]

Vertical Flow Regime Maps

The regimes of gas-liquid flow are a little different when the pipe is oriented vertically as shown in Figure 5.

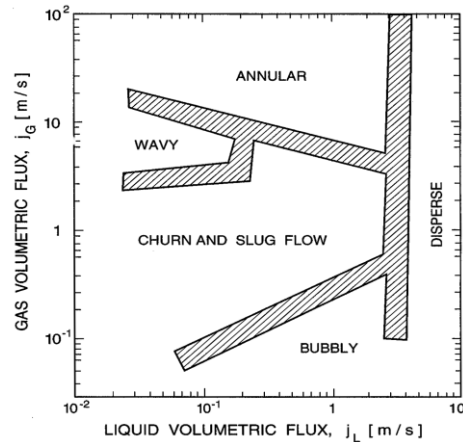


FIGURE 5. A flow regime map for the flow of an air/water mixture in a vertical, 2.5 cm diameter pipe showing the experimentally observed transition regions hatched [4].

2. Parameters affecting the flow regime transition

There are several parameters affecting the flow regime transition. Some of them are given below.

Diameter effect

Lin and Hanratty (1987) [7], and Jepson and Taylor (1993) [8], investigated diameter effect for flow regime transition. The experiments were performed with three different pipes, with the length of 15.5m, 24.6m and 60m, with a diameter of 2.54 cm, 9.53 cm and 30 cm, respectively. The experiments were performed at atmospheric outlet pressure. It is noted that slug flow has not been observed in larger diameter pipes. The maximum diameter at which Taylor bubbles have been seen is less than 0.1m.

Effect of pipe inclination

Pipe inclination is an important parameter that effects flow regime transition. Small changes in the pipe inclination may have a large effect on the stratified-slug-flow pattern transition, in particular at low gas flow rates. For upward pipe angles, gravity acts in the

opposite direction of the flow and it will develop back-flow and accumulation of liquid. The consequence is the generation of slugs at very low liquid flow rates. For downward pipe angles, gravity works in the same direction as the flow, and the result is an increased tendency towards liquid phase stratification, where a higher liquid flow rate is required to form slugs than for horizontal pipes.

Effect of pressure

In high-pressure, gas-liquid flow, complex flow regimes occur at lower gas flow rates. High pressures also increased the tendency towards liquid transport as entrained droplets (Nuland and Lingelem, 1993) [9]. As a result of this, the average liquid holdup decreases, and which again reduces the possibility for generation of stable slugs.

The viscosity of the liquid

Flow types are determined by stability, and viscosity is one of the factors that affect instability. With increasing liquid viscosity, the liquid height (critical liquid height) at the transition increases.

Stability of flow regimes

Flow types are determined by stability. As the flow parameters change, some types of flow lose and others gain stability. The theory of stability is the way to analyze the transition between two types. Instability can be caused by different reasons. Some of them are given below [10].

- . Viscosity stratification
- . Density stratification
- . Velocity profile curvature
- . Shear effects in one of the constitutive phase

There are two main instabilities in multiphase flow, i.e. Kelvin-Helmholtz instability and Rayleigh-Taylor instability.

3. Objectives

The objective of this project is to characterize flow regimes in air-water two-phase flow based on pressure and density measurements and find the criteria for the transition between flow regimes using pressure and density parameters. Then the parameters are to be

compared with the existing experimental models in order to verify the criteria.

4. Experimental procedure

The experiments were performed by setting the liquid flow rate constant and varying the gas flow rates (Figure 6). First, the water flow rate was set to 12 and the gas flow rate to 20. At the steady state, density and the pressure data are recorded for 10 min and the flow regime was observed visually and recorded. Keeping the liquid flow rate constant at 12, the gas flow rate was changed to 30. Pressure and density data were recorded as the previous one. The experiment was repeated by changing the gas flow rate by the difference of 10 to 90 and vice versa. The second test series were done with liquid flow rate at 8 and the gas flow rate to 70. As the steady state was reached the density and pressure were recorded. Similarly as before the experiment was repeated by changing the gas flow rate by the difference of 10 to 90 and then in the reversed direction as well. Finally, the liquid flow rate was set to 4 and the gas flow rate to 70. Again density and pressure were recorded. As before, the experiment was repeated by changing the gas flow rate by the difference of 10 to 80 and then in the reversed direction as well. The test matrix is given in Table 1 with the visual observations.

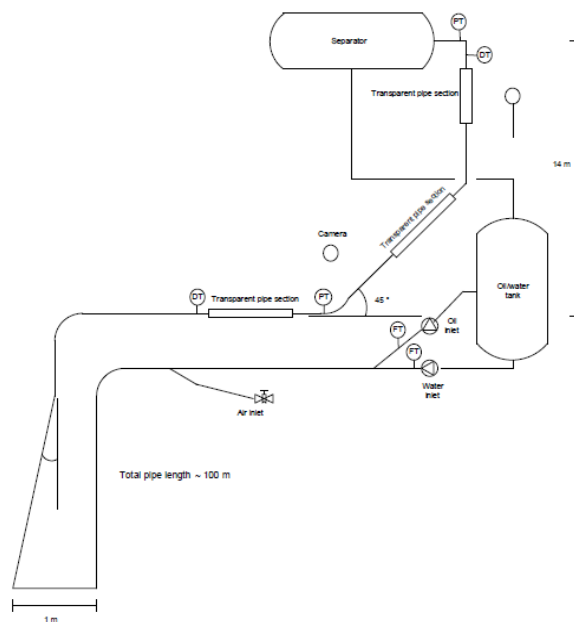


FIGURE 6. Sketch of the test rig.

TABLE 1. Test matrix of the experiments at the test rig

Test ID	Gas flow rate	Liquid flow rate	Visual Observation
AW 20/12	20	12	Slug/bubble
AW 30/12	30	12	Slug/bubble
AW 40/12	40	12	Slug
AW 50/12	50	12	Slug
AW 60/12	60	12	Slug
AW 70/12	70	12	Slug
AW 80/12	80	12	Slug
AW 90/12	90	12	Slug
AW 70/8	70	8	Slug
AW 80/8	80	8	Slug/Churn
AW 90/8	90	8	Slug/Churn
AW 70/4	70	4	Slug/Churn
AW 80/4	80	4	Slug/Churn

Time series analysis of density and pressure

Simultaneous analysis of multiple time series require some degree of automation, due to a large amount of data involved. For one experiment, four-time traces were analyzed, each containing up to 1000-12000 samples. An analysis software was implemented in MATLAB, and the Graphical User Interface (GUI) is shown in Figure 7. The main motivation for generating a software simulation was to ensure equal treatment of all data points and to interactively be able to evaluate and modify the automatic calculations.

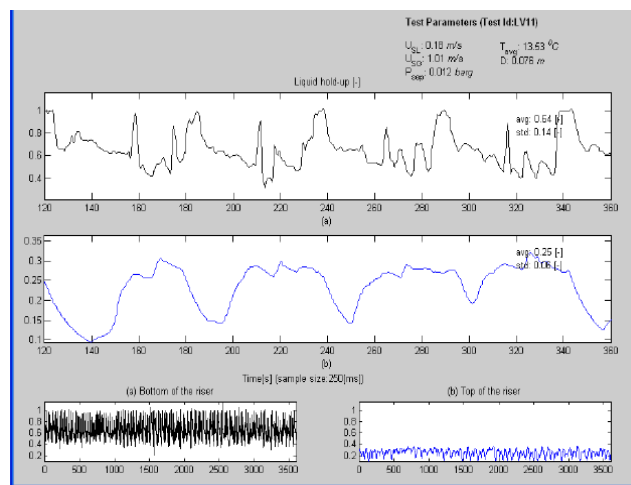


FIGURE 7. GUI of the time domain analysis of the time series data of experiments

Figure 7 shows the liquid holdup and pressure measurements over a period of 240 seconds at a specific flow rate. The graph at the bottom in figures represents the conditions at the

top of the riser, while the graph at the top of the figure represents the conditions at the bottom of the riser.

The plot in Figure 8 is from a test series the project group have performed. The liquid flow rate is 12 and the gas flow rate is 90. The flow pattern has changed totally compared to the previous experiment. The plot shows pulsating flow with about 5 seconds between each dense liquid peak. The average liquid holdup at the bottom of the riser is 0.63, and 0.26 at the top. The frequencies of the dense liquid peak are quite even between the top and bottom of the riser.

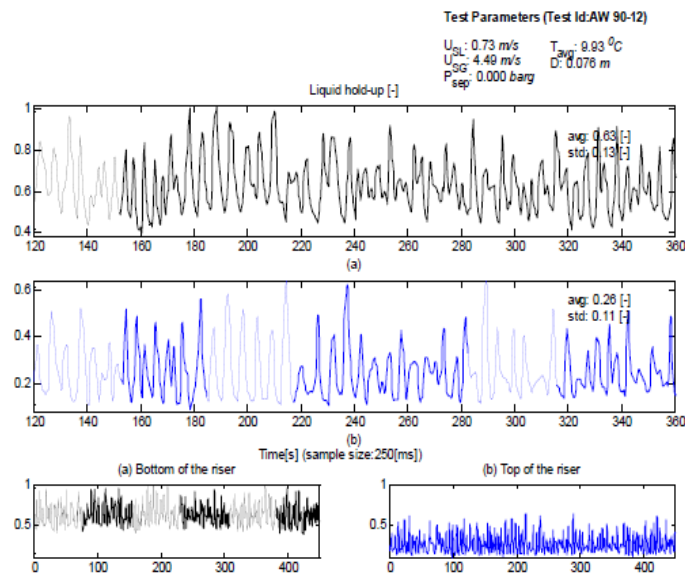


FIGURE 8. The liquid hold up of AW 90/12

Figure 9 is the pressure plot from the same experiment and shows that the deviation at the bottom of the riser is 100 mbar, and 240 mbar at the top of the riser. It is pulsating flow, with the same high frequency of the pressure peaks as in the holdup plot. The standard deviation is very high at the top of the riser, 121 mbar. This is high, compared with the previous two experiments which have 16 mbar and 75 mbar respectively.

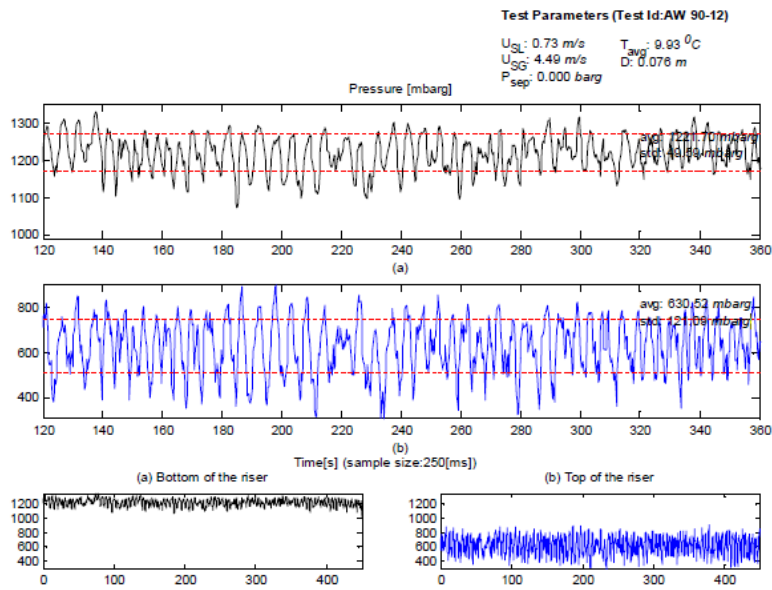


FIGURE 9. Pressure analysis of AW 90/12

The plots in Figure 10 are from an experiment where the liquid flow rate was kept constant, and the 30 gas flow rate was reduced to 30. The average liquid holdup at the bottom of the riser is 0.85, and 0.43 at the top. The frequency between the dense peaks is around 7.5 seconds and is reduced by 50% from the previous flow rate. By reducing the gas velocity from 90 to 30, the liquid holdup at the bottom was increased from 0.63 to 0.85 and from 0.26 to 0.43 at the top.

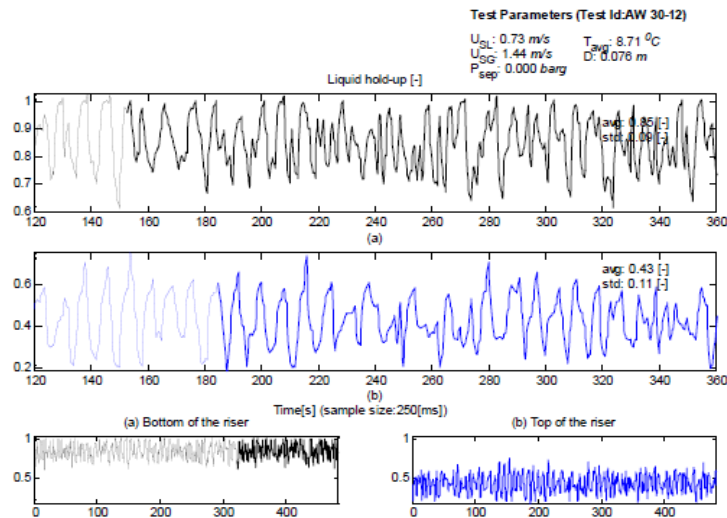


FIGURE 10. Liquid hold-up analysis of AW 30/12

The corresponding pressure diagram is shown in Figure 11. The pressure deviation at the bottom and top of the riser is 1178 mbar and 312 mbar respectively. By reducing the gas flow rate, the pressure at the top of the riser has been reduced by approximately 50%, from 626 mbar to 312 mbar.

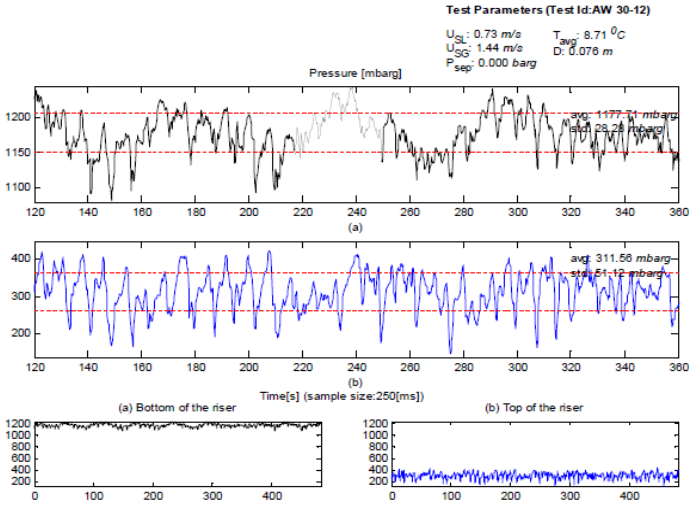


FIGURE 11. Pressure analysis of AW 30/12

The plot in Figure 12 is from an experiment with a liquid flow rate of 4, and a gas flow rate of 70. The frequency between the dense peaks is about 10 seconds and is evenly divided over the whole period. The average liquid holdup at the bottom is 0.53 and 0.16 at the top. The standard deviation at the bottom and the top are 0.1 and 0.07 respectively.

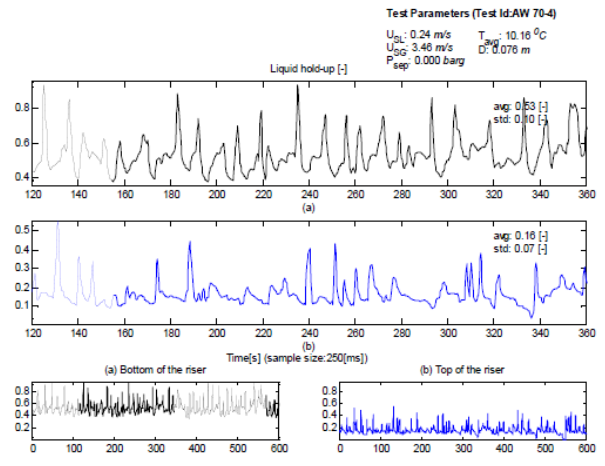


FIGURE 12. Liquid hold-up analysis of AW 70/4

The corresponding pressure diagram is shown in Figure 13, and the pressure at the bottom

of the riser is 560 mbar and 162 mbar at the top. The pressure deviation is 124 mbar at the bottom of the riser, and 136 mbar at the top.

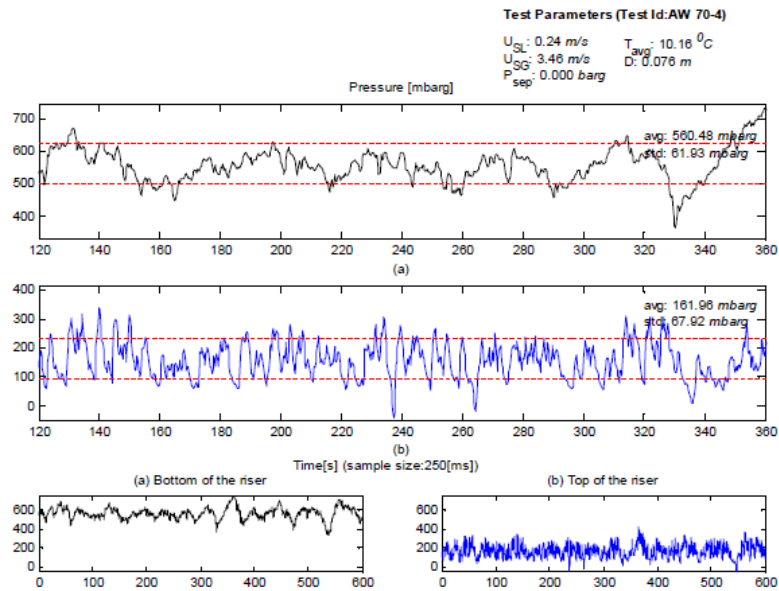


FIGURE 13. Pressure analysis of AW 70/4

The plot in Figure 14 is shown the frequency domain analysis of the experiment of AW 70/4.

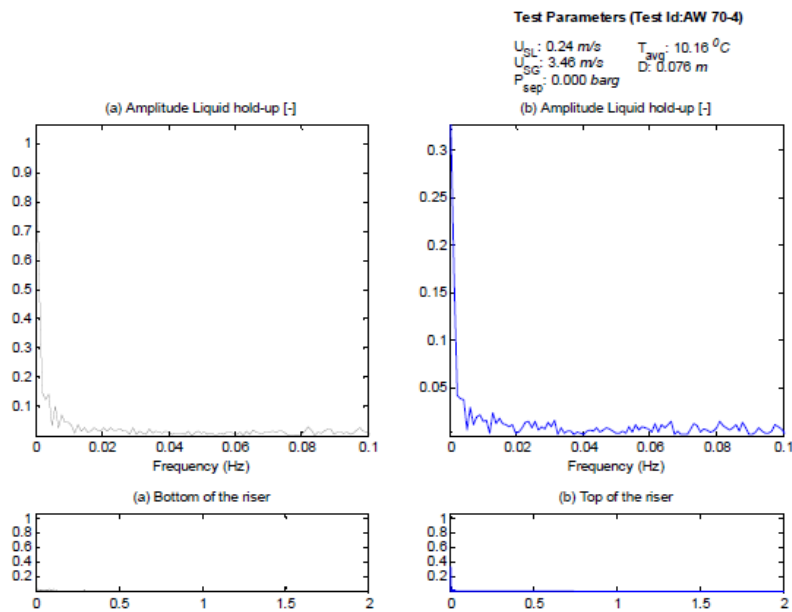


FIGURE 14. Frequency domain analysis of liquid holdup of AW 70/4

For all experiments conditions, liquid hold up and pressure difference values are given in

Table 2. According to the developed figures for pressure drop and liquid hold up, selected the boundary values. If the bottom of the riser liquid hold up is between 0.62 - 0.72 and pressure difference is approximately 107 mbar, then it can be observed as slug flow.

TABLE 2. Flow regime evaluation based on flow regime criterion

Test ID	Avg. H _L (bottom)	Avg. H _L (top)	ΔP(bottom)	ΔP(top)	Flow regime based on flow regime criteria
AW 20/12	0.86	0.49	65	100	-
AW 30/12	0.85	0.43	57	102	-
AW 40/12	0.79	0.38	65	142	-
AW 50/12	0.74	0.34	75	173	-
AW 60/12	0.72	0.32	87	201	Slug
AW 70/12	0.68	0.30	83	204	Slug
AW 80/12	0.66	0.28	96	227	Slug
AW 90/12	0.63	0.26	99	242	Slug
AW 70/8	0.60	0.23	97	182	-
AW 80/8	0.56	0.21	90	190	-
AW 90/8	0.54	0.20	97	208	-
AW 70/4	0.53	0.16	124	138	-
AW 80/4	0.51	0.14	184	167	-

5. Comparison with experimental models

Results are compared with the simple experimental models from the literature. Some parameters are not exactly matching with test rig properties, i.e. diameter of the pipe. The experimental results are applied to the models with assumptions.

1. Entrance effect mechanism

According to Dukler & Taitel (1986) the actual pipe length, l is less than the entrance length, l_e then churn flow may be observed in the entire pipe. Otherwise, slug flow will be observed at the end of the pipe. Entrance length for all the experiments is calculated according to Equation 1 and listed in Table 3. Since the actual pipe length is $l = 14\text{m}$ for the test rig, this method gives a slug flow for all the experiments. These results are quite similar to the results that are found from the visual observation.

$$\frac{l_e}{D} = 42.6 \left(\frac{U_m}{\sqrt{gD}} + 0.29 \right) \quad (1)$$

Where U_m is the mixture velocity, i.e. the sum of the superficial velocities of the two phases, g is the acceleration due to gravity and D is the tube inner diameter. If the actual pipe length is less than l_e calculated using the above equation, then churn flow may be observed in the entire pipe; otherwise, slug flow will be observed at the end. (Dukler, A.E. and Taitel, Y., 1986)

TABLE 3. Flow regime evaluation for the experiments according to Dukler & Taitel (1986) entrance effect mechanism.

Test ID	Q_G	Q_L	l_e	Visual Observation
AW 20/12	20	12	5.38	Slug
AW 30/12	30	12	6.24	Slug
AW 40/12	40	12	7.10	Slug
AW 50/12	50	12	7.94	Slug
AW 60/12	60	12	8.82	Slug
AW 70/12	70	12	9.65	Slug
AW 80/12	80	12	10.43	Slug
AW 90/12	90	12	11.19	Slug
AW 70/8	70	8	9.91	Slug
AW 80/8	80	8	10.96	Slug
AW 90/8	90	8	11.99	Slug
AW 70/4	70	4	10.18	Slug
AW 80/4	80	4	11.37	Slug

2. Wake effect of Taylor bubbles

According to Mishima & Ishii (1984) transition from slug to churn flow occurs when the void fraction in the pipe, ϵ_{avg} is just greater than the mean void fraction over the Taylor bubble region ϵ_b . The calculations of void fraction in the pipe and mean void fraction over the Taylor bubble region values for all the experiments according to the model given in Equation 2 and 3 are listed in Table 4.

$$\epsilon_{avg} = \frac{U_{GS}}{C_o U_m + 0.35 \sqrt{\frac{\Delta \rho g D}{\rho_L}}} \quad (2)$$

and

$$\epsilon_b = 1 - 0.813 \left[\frac{(C_o - 1) U_m + 0.35 \sqrt{\frac{\Delta \rho g D}{\rho_L}}}{U_m + 0.75 \sqrt{\frac{\Delta \rho g D}{\rho_L}} \left(\frac{\Delta \rho g D^3 \rho_L}{\mu_L} \right)^{\frac{1}{18}}} \right]^{\frac{3}{4}} \quad (3)$$

Where,

$$\Delta\rho = \rho_L - \rho_G$$

$$C_o = 1.2 - 0.2 \sqrt{\frac{\rho_G}{\rho_L}} \text{ for round tubes}$$

$$C_o = 1.35 - 0.35 \sqrt{\frac{\rho_G}{\rho_L}} \text{ for rectangular tubes}$$

$$U_m = U_{GS} + U_{LS}$$

The normal value for μ_L (liquid viscosity) is 0.001 Ns/m²

TABLE 4. Flow regime evaluation for the experiments according to the wake effect of Taylor bubbles.

Test ID	Q _G	Q _L	ϵ_{avg}	ϵ_b	Visual Observation
AW 20/12	20	12	0.26	0.80	Slug
AW 30/12	30	12	0.34	0.80	Slug
AW 40/12	40	12	0.40	0.80	Slug
AW 50/12	50	12	0.45	0.80	Slug
AW 60/12	60	12	0.49	0.79	Slug
AW 70/12	70	12	0.52	0.79	Slug
AW 80/12	80	12	0.54	0.79	Slug
AW 90/12	90	12	0.56	0.78	Slug
AW 70/8	70	8	0.60	0.80	Slug
AW 80/8	80	8	0.63	0.79	Slug
AW 90/8	90	8	0.65	0.79	Slug
AW 70/4	70	4	0.69	0.79	Slug
AW 80/4	80	4	0.70	0.79	Slug

3. Slug collapse by bubble coalescence

Brauner & Barnea (1986) found that when the void fraction in the liquid slug, ϵ_s reaches 0.52, the bubbles get coalesce which destroys the identity of the liquid slug and leads to churn flow. Thus, the transition to churn flow occurs when $\epsilon_s > 0.52$. The void fraction in the liquid slug, ϵ_s for all the experiments are calculated according to Equation 4 and listed in Table 5. It is shown that the values of ϵ_s are 0.2 which is less than the transition condition. Therefore all the experiments are shown slug flow according to this model.

The expression for a void fraction in the slug, ϵ_s for given flow condition is as follows:

$$\epsilon_s = 0.058 \left[d_c \left(\frac{2f_m U_m^3}{D} \right)^{0.4} \left(\frac{\rho_L}{D} \right)^{0.6} - 0.725 \right]^2 \quad (4)$$

Where d_c is the characteristic bubble size which for vertical flow is given by,

$$d_c = 2 \sqrt{\frac{0.4\sigma}{g\Delta\rho}} \quad (5)$$

Here σ is the surface tension and f_m is the friction factor based on the mixture velocity, U_m , and is defined as

$$f_m = \frac{2T_w}{\rho_L U_m^2} \quad (6)$$

Where T_w is the wall shear stress. The friction factor is obtained from the usual f vs Re relationships, with the Reynolds number being defined as,

$$Re = \frac{\rho_L U_m D}{\mu_L} \quad (7)$$

$$f_m = \frac{16}{Re} \quad \text{if } Re \leq 2100$$

$$f_m = 0.046 Re^{-0.2} \quad \text{if } Re > 2100$$

Normally surface tension for air-water flow is 0.072 N/m.

TABLE 5. Flow regime evaluation for the experiments according to slug collapse by bubble coalescence.

Test ID	Q_G	Q_L	ϵ_s	Flow regime
AW 20/12	20	12	0.02	Slug
AW 30/12	30	12	0.02	Slug
AW 40/12	40	12	0.02	Slug

AW 50/12	50	12	0.01	Slug
AW 60/12	60	12	0.02	Slug
AW 70/12	70	12	0.02	Slug
AW 80/12	80	12	0.01	Slug
AW 90/12	90	12	0.02	Slug
AW 70/8	70	8	0.01	Slug
AW 80/8	80	8	0.01	Slug
AW 90/8	90	8	0.01	Slug
AW 70/4	70	4	0.01	Slug
AW 80/4	80	4	0.01	Slug

4. Owen's experimental results

Owen (1986) has built a table of flow regime transition in air-water vertical upward flow at a test section pressure of 2.4 bar and pipe diameter $D = 0.0318\text{m}$ as shown in Table 6. Once the liquid mass flux is known, then it gives the boundary values of gas mass flux at the flow regime transition between bubbly to slug and slug to churn. Some of the liquid mass flux data of the experiments are out of Owen's data range. Therefore Owen's flow regime criteria table is extended for the experimental mass fluxes using interpolation and extrapolation.

TABLE 6. Owen's experimental results for flow regime transition based on mass fluxes

Liquid mass flux	Gas mass flux at the flow regime transition between	
	<i>Bubbly & Slug</i>	<i>Slug & churn</i>
5.3	5.8	6.5-8.0
10.3	5.9	7.1-9.0
49.5	5.9	8.2-9.6
111.8	5.8	9.6-11.3
199	4.6	6.6-8.4
297	4.6	9.0-14.3
399	-	11.3-13.4
182*	4.6	6.4
243*	4.6	7.8
487*	-	13.3
548*	-	14.7
731*	-	18.8
914*	-	22.9

*extended mass fluxes

Evaluation of the flow regime based on the extended Owen's flow regime criteria is listed in Table 7. According to Owen (1986), slug to churn transition occur when the gas mass

flux of 18.8 for the liquid mass flux of 731.3. But the maximum liquid flux and the gas flux that can be obtained from these experiments are 731.3 and 5.48 respectively. As the transition conditions for the mass fluxes are higher than the obtained values, slug to churn cannot be achieved from these flow conditions.

TABLE 8. Flow regime evaluation for the experiments based on Owen's experimental results and extended Owen's results.

Test ID	Q_G	Q_L	Liquid mass flux	Gas mass flux	Flow regime
AW 20/12	20	12	731.31	1.22	Slug
AW 30/12	30	12	731.31	1.83	Slug
AW 40/12	40	12	731.31	2.44	Slug
AW 50/12	50	12	731.31	3.05	Slug
AW 60/12	60	12	731.31	3.66	Slug
AW 70/12	70	12	731.31	4.27	Slug
AW 80/12	80	12	731.31	4.88	Slug
AW 90/12	90	12	731.31	5.48	Slug
AW 70/8	70	8	487.53	4.27	Slug
AW 80/8	80	8	487.53	4.88	Slug
AW 90/8	90	8	487.53	5.48	Slug
AW 70/4	70	4	243.77	4.27	Bubble
AW 80/4	80	4	243.77	4.88	Slug

6. Discussion

The flow regime criteria that is developed based on the analysis of experimental data is compared with existing experimental models for air-water flow. The experimental data are applied to five different methods of a slug to churn transition criteria based on assumptions. A discussion about the comparison is given in the following section.

Entrance effect mechanism

According to the entrance effect mechanism, if the actual pipe length is less than le calculated using Equation 1, then churn flow may be observed in the entire pipe, otherwise, slug flow will be observed at the end. This model gives slug flow for all the experiments. But the experiments of water flow rate 4 and 8 are visually observed as churn flow. However, this theory has been developed for 2.5 cm and 5 cm pipes. The test rig has a pipe diameter of 7.6 cm. This diameter difference might be affected to the results.

Wake effect of Taylor bubbles

According to this mechanism, slug to churn flow occurs when the void fraction in the pipe, ϵ_b is slightly greater than the mean void fraction over the Taylor bubble region, ϵ_{avg} . This model gives slug flow for all the experiments. Accuracy of this method depends on the liquid flow rate. The liquid flow rates used in the experiments can be assumed as low flow rates for this method. (Exact boundary conditions for low, medium and high flow rates have not been defined by the author). The author has done this experiment for different diameter, but it can be used for other diameters as well because the diameter is one parameter in the model. Therefore by neglecting those small differences, this method gives a good prediction for proving experimental data.

Slug collapse by bubble coalescence

According to the theory, transition to churn flow occurs, when void fraction in the liquid slug is greater than 0.52. This is based on the assumption that the gas in the liquid slug behaves as dispersed bubbles because of the turbulence within the slug. The experimental flow rates in this project can be considered as low flow rates. This is probably the reason why it gives very small values for ϵ_b even boundary value should be 0.52. All the calculated value of ϵ_b for experimental data are in the range of 0.01 - 0.03. Therefore all values are less than 0.52 and give slug flow. The values are very small, therefore even it is proven that observations are correct, values are unrealistic. It can be mentioned that this method cannot be accurate for low liquid flow rates. (Exact boundary conditions for low, medium and high flow rates have not been defined by the author)

Owen's experimental results

The author has performed experiments at different experimental conditions and he has not performed for liquid mass flux higher than 399. Therefore it is not possible to compare experimental flow rates with this method. The required gas mass fluxes were calculated using extrapolation and interpolation to extend Owen's mass flux data. Extended Owen's data are used to compare with experimental liquid mass fluxes. The calculated gas mass fluxes of the experiments are not in the range of transition from slug to churn, i.e. when the

liquid mass flux is 487, the maximum gas mass flux was 5.5. But for the slug to churn transition it should be 13.3. Therefore this method gives slug flow. Since the industry interests on liquid and gas mass fluxes for slug flow, this method gives important boundary conditions for a bubble to slug and slug to churn transition.

Discussion of the plots and results from the model

According to the boundary condition, the average liquid holdup, at the bottom of the riser, should be in the range 0.62 - 0.72 and the pressure deviation at the bottom of the riser should be approximately 107 mbar to register slug flow. The average liquid holdup and the pressure deviations for the same experiments as the plots in Chapter 4 are shown in Table 9.

TABLE 9. Holdup and pressure differences for the chosen experiments

Test ID	Avg. H _L (bottom)	Avg. H _L (top)	ΔP(bottom)	ΔP(top)
AW 30/12	0.73	0.43	99.2	102.2
AW 90/12	0.63	0.26	56.6	242.2
AW 70/4	0.53	0.16	124	136

Table 10 shows the comparison between pressure and liquid holdup boundary conditions, with different models. After applying the boundary conditions to the different experiments, and comparing with the different models, some inconsistency can be seen.

TABLE 10. Classification of flow regimes for chosen experiments and comparison with experimental models

Test ID	Based on flow regime criteria	Visual Observation	Entrance effect	Wake effect	Slug col. by bubble coal.	Owen's experimental results	Flow regime map
AW 30/12	No slug	Bubble/Slug	Slug	Slug	Slug	Slug	Slug
AW 90/12	Slug	Slug	Slug	Slug	Slug	Slug	Slug
AW 70/4	No slug	Slug/Churn	Slug	Slug	Slug	Bubble	Churn

The project group has not been able to define any boundary conditions for a liquid holdup at the top of the riser. However, it should be possible to apply the pressure criterion, but for

these four experiments, it will not have any influence on the flow regimes listed in Table 10. When comparing the experiments the project group have performed with experiments performed by Statoil, it can be observed that higher liquid and gas velocity gives higher frequency and shorter time between the slugs. This is one parameter which pointing in the direction of churn flow. Although, many of the experiment that the project group has been considering, most of them points in the direction of slug flow, but the above-mentioned case could imply churn flow.

Suggestions for further studies

- Slug to churn transition may obtain when the liquid flow rate is 4 and gas flow rate 90 or 100 (90/4; 100/4). Also at liquid flow rate 8 and gas flow rate 100 (100/8).
- Bubble to slug transition may obtain when the liquid flow rate 3 and gas flow rate 5 - 15. Liquid flow rate 12 and gas flow rate 5 - 30 may also give bubble to slug transition.
- For more accurate flow regime observations, recommend using high frame rate video cameras.
- Several parameters of statistical analysis should be investigated to improve the flow regime transition criteria.
- Parameters in both horizontal and vertical pipe flow should be investigated for the transition criteria.
- It would be better to validate the flow regime criteria by changing parameters that affect the transition.

Conclusion

The physical understanding of multiphase flow characteristics in vertical and horizontal pipes is of great importance to the petroleum industry. Slug flow is a complex type of flow with an unsteady nature, thus the prediction of the flow conditions are difficult. Slug to churn transition in vertical flow is a complex fluid mechanical problem, which has turned out to be a difficult task to solve. The test series consists of 13 different flow rates of air and water. Time series analysis of the liquid holdup and pressure differences, as well as video recording and visual observation, has been used to characterize the flow regime and find boundary condition for flow regime transition. The project group has defined boundary condition values for the average liquid hold up and pressure difference based on several

flow tests. The average liquid hold up at the bottom of the riser should be in the range of 0.62-0.72, and the pressure difference is approximately 107 mbar. If both of the above conditions are satisfied, then the flow regime should be a slug.

REFERENCES

- [1] L. Cheng, G. Ribatski, J. R. Thome, Two-Phase Flow Patterns and Flow-Pattern Maps: Fundamentals and Applications, *Applied Mechanics Reviews*, Vol. 61, 1-28, 2008,
- [2] Z. Li, G. Wang, Muhammad Yousaf, Xiaohong Yang, Mamoru Ishii, Flow structure and flow regime transitions of downward two-phase flow in large diameter pipes, *International Journal of Heat and Mass Transfer*, 118, 812-822, 2018.
- [3] I. M. Vaillancourt, K. Pehlivan, Two-Phase Flow Regime Transitions in Microchannels: A Comparative Experimental Study, *Microscale Thermo physical Engineering*, 9(2):165-182, 2005.
- [4] E.B. Christopher, Fundamentals of Multiphase Flows. Cambridge University Press, 163-194, 2005.
- [5] C.P. Fairhurst, Upward Vertical Two-Phase Flow through an Annulus, *Multi-Phase Flow Proceedings of the 4th International Conference* : Chapter 20, 1989.
- [6] U. Kadri, R.F. Mudde, R.V.A. Oliemans, M. Bonizzi and P. Andreussi: Prediction of the transition from stratified to slug flow or roll-waves in gas-liquid horizontal pipes, *International Journal of Multiphase Flow* , 35, Issue 11, 1001-1010. 2009.
- [7] W.P.Jepson, R.E.Taylor, Slug flow and its transitions in large-diameter horizontal pipes, *International Journal of Multiphase Flow*, Volume 19, Issue 3, Pages 411-420, June 1993.
- [8] P.Y. Lin, T.J. Hanratty, Effect of Pipe Diameter on Flow Patterns for Air-Water Flow in Horizontal, *International Journal of Multiphase Flow*, 13(4):549-563, 1987.
- [9] L.I. Ryabova, N.B. Savenok. N.A. Mariampolskij, L.M. Surova, D.F. Kovalev. Plugging solution-contains Portland cement, alu-minium oxychloride, water and phosphonium complexone in form of e.g., oxy-ethylidene diphosphonic acid. Patent: SU 1802086-A, 1993.
- [10] P.A.M. Boomkamp, R.H.M Miesen, Classification of instabilities in parallel two-phase flow. *Int. J. Multiphase Flow*, Vol. 22, 67-88, 1997.
- [11] A.E. Dukler, Y. Taitel, Flow pattern transition in gas-liquid systems: measurement and modeling. *Multiphase science and technology*, Vol. 2, 1-94, 1986.
- [12] K. Mishima, I. Ishii, Flow regime transition criteria for two-phase flow in vertical tubes. *Int. J. Heat Mass Transfer*, Vol. 27, 723-734, 1984.
- [13] N. Brauner, D. Barnea, Slug/Churn transition in upward gas-liquid flow. *Chem. Engng Sci.* Vol. 41, 159-163, 1986.
- [14] D. G. Owen, An Experimental and Theoretical Analysis of Equilibrium Annular Flows, PhD Thesis, University of Birmingham, 1986.